CARBONATE MELT LITHOLOGIES FROM THE STEINHEIM IMPACT CRATER (SW GERMANY).
D. Anders[1], P. Kegler[1], E. Buchner[2,3] and M. Schmieder[3], [1]Institut für Geowissenschaften, Christian-Albrechts-Universität zu Kiel, Germany (denise.anders@hotmail.de; phk@min.uni-kiel.de), [2]HNU Neu-Ulm University, Germany, [3]Institut für Planetologie, Universität Stuttgart, Germany (elmar.buchner@geologie.uni-stuttgart.de; martin.schmieder@geologie.uni-stuttgart.de).

Introduction: The ~3.8 km Steinheim impact structure, hosted by a thick suite of Triassic to Upper Jurassic sedimentary rocks of the Swabian Alb plateau (SW Germany), counts among the best-preserved small, complex impact structures with central uplift on Earth [1;2]. Although studied for decades and intensely drilled since the 1960s [3], no impact melt lithologies were known from this impact crater until the recent report of melt-bearing suevitic impact breccias in the B-26 drill core [2]. We newly investigated this core drilled in the western central annular basin of the Steinheim Basin in the search for potential new carbonatic melt lithologies (compare [4]).

Samples and Analytical Methods: The B-26 drill core analyzed in this study was recovered from the western annular moat of the Steinheim Basin (48°41’13’’N, 10°03’27’’E) in 1979. Polished thin sections of B-26 drill core material were examined by petrographic microscopy. Backscattered electron (BSE) images were made on a CamScan SC44 scanning electron microscope (SEM) in order to characterize microstuctures. Chemical analyses were carried out using a CAMECA SX-100 electron microprobe (University of Stuttgart).

Results: An optical and SEM-based reinvestigation of microscopic impact melt particles (Fig. 1 a) in the B-26 core (carbonatic suevitic impact breccia at depth 76-77 m) revealed numerous minute, droplet- to diapir-shaped, partially fluidal, and rarely honeycomb-textured Ca-carbonate domains (Fig. 1 b, c, d) accompanied by monomineralic, fluidal silica patches, and spinifex-textured Fe-Ni-Co sulfides), embedded in melt particles largely transformed into phyllosilicates [2]. The silicate-calcite contact is sharp but locally intented showing curved menisci and extensions budding into the silicate melt. SEM-EDX analyses yielded an essentially pure calcite composition of the monomineralic Ca-carbonate melt patches. Similar impact breccias were encountered in shallower, coherent parts of the B-26 core (46-48 m and 52-53 m, respectively).

At a depth of 78-79 m, closely beneath the structural crater floor of the Steinheim Basin, the B-26 drill core consists of fractured and brecciated parautochthonous Upper Jurassic limestone of the subcrater target rock. Macroscopic fractures in the limestone are filled with brownish, partially fluidally-textured veins of Ca-Mg-carbonates (Fig. 2).

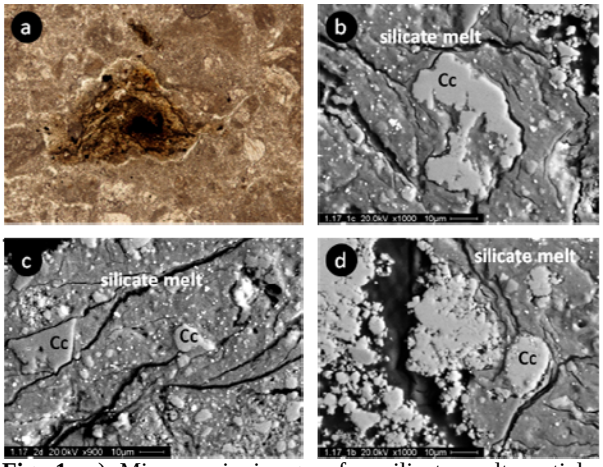

Fig. 1: a) Microscopic image of a silicate melt particle within the Steinheim impact breccia showing fluidal textures (particle size ~500 µm; plane-polarized light). BSE images of b) diapiric calcite (Cc) particle embedded in the silicate melt matrix, displaying features of silicate-carbonate liquid immiscibility. c) Calcite globule within a silicate melt particle. d) Droplet-shaped calcite particle.

Fig. 2: Thin section scan of clast-rich carbonate crack fillings (dark) within the subcrater target limestone (bright), showing relicts of an overall fluidal texture of the vein.

Numerous calcitic and minor dolomitic clasts, set into a ‘dolomitic’ Ca-Mg-carbonate groundmass composed of crypto- to microcrystalline aggregates (Fig. 3 a, b) and poor in vesicles, are commonly well-rounded (in some cases nearly spherical to lenticular), often show ‘crackeled’ textures, and are marginally decomposed into micro- to cryptocrystalline aggregates of Ca-Mg-carbonates or intersected by microcracks that are filled with carbonate groundmass (Fig. 3 c, d).

Electron microprobe and SEM-EDX measurements yielded detectable enrichment in Al and Si (locally >3 wt% Al_2O_3 and SiO_2 in total), dominant in interstices forming a reticular pattern within the dolomitic groundmass with MgO contents of up to ~20 wt%. The vein groundmass is, furthermore, host to idiomorphic and spherule-shaped Fe-sulfides and rare, micrometer-sized, Fe-Ni spherules with nickel contents of up to 1.77 wt% (compare [2;6]).

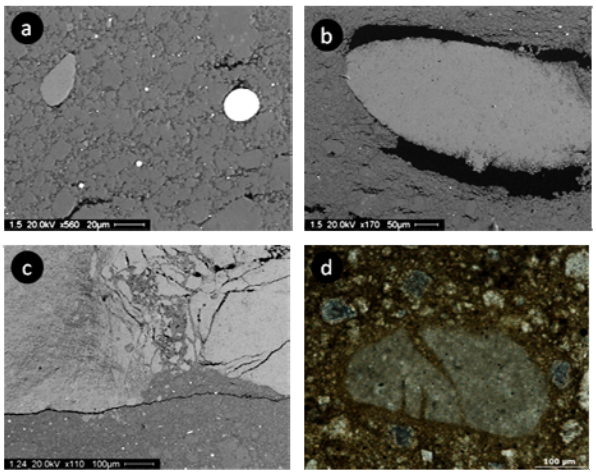

Fig. 3: BSE images of a) cryptocrystalline dolomitic groundmass of the carbonate vein filling; note well-rounded calcitic clast (left) and spherule-shaped Fe-sulfide (right). b) Well-rounded calcitic limestone clast within the carbonate groundmass. c) Injections of the carbonatic vein groundmass into microfractures in partially decomposed calcitic limestone clasts. d) Microscopic picture of cracks within a calcite clast filled with dolomitic groundmass (cross-polarized light).

Interpretation: The microtextural features of the monomineralic calcite domains within the silicate melt particles provide evidence of originally liquid phases and silicate-carbonate-liquid immiscibilty. The textural characteristics of these melt domains suggest that calcitic limestone (or larger calcite crystals) as constituents of the target rock were molten upon impact (Fig.1; see also [2] and compare recent review by [5]).

The petrographic characteristics of the fluidal Ca-Mg-carbonatic veins and clasts therein (Fig. 2) suggests that they formed as local carbonate-domainated melts, injected into open target rock fractures. This interpretation is in accord with the admixture of Ni-rich spherules presumably inherited from the (iron meteoritic?) Steinheim impactor [2;6], the crystallization of idiomorphic and spherule-shaped Fe-sulfides from a liquid, the marginal melting and decomposition (thermal corrosion and/or degassing) of limestone clasts (Fig. 3 a, b), the injection of the vein groundmass material into SEM-scale microfractures within the adjacent wall rock limestone (Fig. 3 c, d), and the incorporation of resolvable amounts of Si and Al into the Ca-Mg-carbonate groundmass [7]. Based on phase relationships of dolomite dependent on pressure, temperature, and composition (e.g., [8]), the dolomitic melt assemblage with MgO contents of up to ~20 wt% (~40 wt% $MgCO_3$) might have formed on a retrograde path at pressures of about 2.7 GPa.

Conclusions: Based on our observations on the B-26 drill core, we conclude that the Steinheim impact produced smaller amounts of carbonate melts, either as monomineralic calcitic patches within mixed-melt particles in the Steinheim suevite (Fig. 1), or as veins of impact melt rocks predominantly generated from dolomitic parts of the Steinheim target rock and subsequently injected into host limestone fractures (Figs. 2 and 3). The occurrence of such melts might be in some analogy to the carbonatic impact melt rocks reported from the larger, ~24 km Haughton impact structure in arctic Canada [7]. A search for periclase (MgO) as a dolomite decomposition product (e.g., [5]) is projected; phase diagrams indicate that lower pressures cause an expansion of the stable percilase field [9]. In context with the generally low pressure estimates for the Steinheim impact event (numerous well-defined shatter cones but very rare shocked quartz grains [2]), which might be ascribed to a distinct 'shock buffering effect' due to a water-saturated, deeply karstified (i.e., highly porous) target in the Miocene [10], it is suggested that shock metamorphism and target rock melting at Steinheim was dominated by comparatively high post-shock temperatures [2].

This abstract is a summary of the first author's B.Sc. thesis [11].

References: [1] Heizmann E. P. J. and Reiff W. (2002) *Der Steinheimer Meteorkrater*. Pfeil, Munich, 160 p. [2] Buchner E. and Schmieder M. (2010) *Meteoritics & Planet. Sci., 45*, 1093–1107. [3] Groschopf P. and Reiff W. (1969) *Geologica Bavarica, 61*, 400-412. [4] Anders D. et al. (2010) *LPSC XLI*, Abstract #1799. [5] Osinski G. R. et al. (2008) *GSA Spec. Pub. 437*, 1-18. [6] Schmieder M. and Buchner E. (2010) *LPSC XLI*, Abstract #2103. [7] Osinski G. R. and Spray J. G. (2001) *EPSL, 194*, 17-29. [8] Wyllie P. J. and Lee W. (1998) *J. Petrol., 39*, 1885–1893. [9] Irving A. J. and Wyllie P. J. (1975) *GCA, 39*, 35-53. [10] Schmieder M. and Buchner E. (2010) *Nördlingen Ries Crater Workshop*, Abstract #7001. [11] Anders D. (2011) B.Sc. thesis, University of Kiel, Germany, 41 p.